On the Design of Stable, High Performance Sigma Delta Modulators

by

Brett Christopher Hannigan

B.A.Sc. (Hons), Simon Fraser University, 2015

A THESIS SUBMITTED IN PARTIAL FULFILLMENT
OF THE REQUIREMENTS FOR THE DEGREE OF

Master of Applied Science

in

THE FACULTY OF GRADUATE STUDIES
(Biomedical Engineering)

The University of British Columbia
(Vancouver)

November 2018

The following individuals certify that they have read, and recommend to the Faculty of Graduate and Postdoctoral Studies for acceptance, the thesis entitled:

On the Design of Stable, High Performance Sigma Delta Modulators

submitted by **Brett Christopher Hannigan** in partial fulfillment of the requirements for the degree of **Master of Applied Science** in **Biomedical Engineering**.

Examining Committee:

Guy Dumont, Electrical and Computer Engineering
Supervisor

Abstract

This document provides brief instructions for using the `ubcdiss` class to write a **UBC!**-conformant dissertation in LaTeX. This document is itself written using the `ubcdiss` class and is intended to serve as an example of writing a dissertation in LaTeX. This document has embedded **URL!**s (**URL!**s) and is intended to be viewed using a computer-based **PDF!** (**PDF!**) reader.

Note: Abstracts should generally try to avoid using acronyms.

Note: at **UBC!** (**UBC!**), both the **GPS!** (**GPS!**) Ph.D. defence programme and the Library's online submission system restricts abstracts to 350 words.

Lay Summary

The goal of this work was a method to better design analog-to-digital converters with special interest to recording weak bio-signals, such as those from electroencephalography and electrocardiography.

The sigma delta architecture of analog-to-digital converters is known for having high resolution for signals of this class while requiring fewer expensive analog circuit components. However, as its performance is increased, it tends to become unstable, a point at which the digitized signal no longer accurately represents the original.

To this end, a theory and set of software tools were developed that use mathematical optimization and control theory to design sigma delta circuits with varying degrees of performance and stability. It is even possible to generate a design that is guaranteed to be stable. The method is generalizable to any kind of signal, medical or otherwise. These developments were used to analyze and synthesize designs and will hopefully inspire future high-resolution analog-to-digital converters.

Preface

At **UBC!**, a preface may be required. Be sure to check the **GPS!** guidelines as they may have specific content to be included.

Table of Contents

List of Tables

List of Figures

List of Symbols

P_Q In-band quantization noise power.

$S(\lambda)$ Sensitivity function.

$T(\lambda)$ Complementary sensitivity function.

Δ Quantization step size.

λ Placeholder for the continuous-time Laplace variable s or discrete-time z-transformation variable z.

e Feedback error signal.

n Filter order.

u Quantizer input signal.

y Digital bitstream output signal.

Glossary

A/D analog-to-digital.

AAF antialiasing filter.

CLANS closed-loop analysis of noise shaper.

CT continuous-time.

D/A digital-to-analog.

DRF digital reconstruction filter.

DT discrete-time.

ECG electrocardiography.

EEG electroencephalography.

FIR finite impulse response.

GKYP generalized Kalman-Yakubovič-Popov.

IIR infinite impulse response.

LF loop filter.

LMI linear matrix inequality.

NTF noise transfer function, equivalent to the sensitivity function.

OSR oversampling ratio.

PPG photoplethysmography.

SQNR signal-to-quantization-noise ratio.

STF signal transfer function, equivalent to the complementary sensitivity function.

Acknowledgments

I would like to thank my supervisor Prof. Guy Dumont for his support of my research and openness to help as well as the other members of the BC Children's Hospital Research Institute's Digital Health Innovation Lab team.

I gratefully acknowledge the funding recieved from industry partner ESS Technologies whose participation in the Mitacs Accelerate program allowed me to write this thesis. The staff at ESS have been especially helpful, many thanks to Martin Mallinson and Chris Petersen in particular whose enthusiastic technical guidance and anecdoes about electronics, mathematics, and the early days of computing were a source of inspiration. Finally, thank you to the others who attended my progress meetings and provided valuable feedback.

Chapter 1

Introduction

The conversion of signals between analog and digital domanis is an often encountered problem in signal processing. For an analog signal to be represented digitally, it must undergo the processes of sampling and quantization (Figure 1.1). The former is the conversion from continuous-time (CT) to discrete-time (DT) and can be done without loss of information by the Nyquist-Shannon sampling theorem, given a sufficiently high sample rate. The latter is the mapping from an infinite set of possible values to a finite number of quantization levels. Unlike sampling, the process of quantization is non-injective and thus irreversible. The design of signal conversion circuits that minimize the error introduced by quantization is a major problem in mixed signal electronics.

Sigma delta modulation is a widely used technique for analog-to-digital (A/D) and digital-to-analog (D/A) conversion of signals that provides high resolution through the techniques of oversampling and noise shaping. Oversampling trades throughput for resolution, thus the sigma delta modulator generally lies between integrating converters, which are specialized for near-dc signals, and high-speed architectures, such as successive approximation and flash. The sigma delta quantization scheme is especially applicable to signals with low to moderate frequency content. Signals with these properties include most biosignals such as those recorded electrically (electroencephalography (EEG), electrocardiography (ECG)) or through other means using transducers (photoplethysmography (PPG)), as well as audio signals.

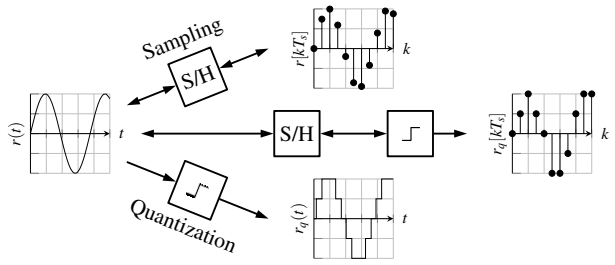

Figure 1.1: A continuous-time, continuous-value signal $r(t)$ is sampled to produce a discrete-time, continuous-value signal $r[kT_s]$. $r(t)$ independently undergoes quantization to yield a continuous-time, discrete-value signal $r_q(t)$. When both processes are applied in sequence, a discrete-time, discrete-value signal $r_q[kT_s]$ is the result.

1.1 Oversampling and Noise Shaping

Oversampling is simply the process where the analog signal is sampled at a rate higher than what the sampling theorem would dictate for perfect reconstruction, expressed as the oversampling ratio (OSR) relative to the Nyquist frequency. It may seem that this does not have a direct benefit *per se*, but it allows a less demanding analog antialiasing filter (AAF) to be used, saving circuit area. It also permits the quantization error to be spread across a larger bandwidth to increase resolution. Assuming quantization error can be modelled by white noise, oversampling reduces the in-band quantization noise power P_Q by a factor directly proportional to OSR [2] as seen in Equation 1.1, where Δ is the difference between quantization levels. These two advantages — reducing analog circuit complexity and increasing resolution — are common goals in sigma delta modulator design.

$$P_Q = \frac{\Delta^2}{12 \cdot OSR} \tag{1.1}$$

It may appear that oversampling alone quickly becomes impractical because one must approach very high sampling frequencies to increase the signal-to-quantization-noise ratio (SQNR) substantially. However, this assumes that the quantization noise is evenly distributed across the spectrum. Noise shaping is the use of a filter operating on the oversampled signal to push quantization noise out of the signal band where it can be removed by digital reconstruction filter (DRF). This

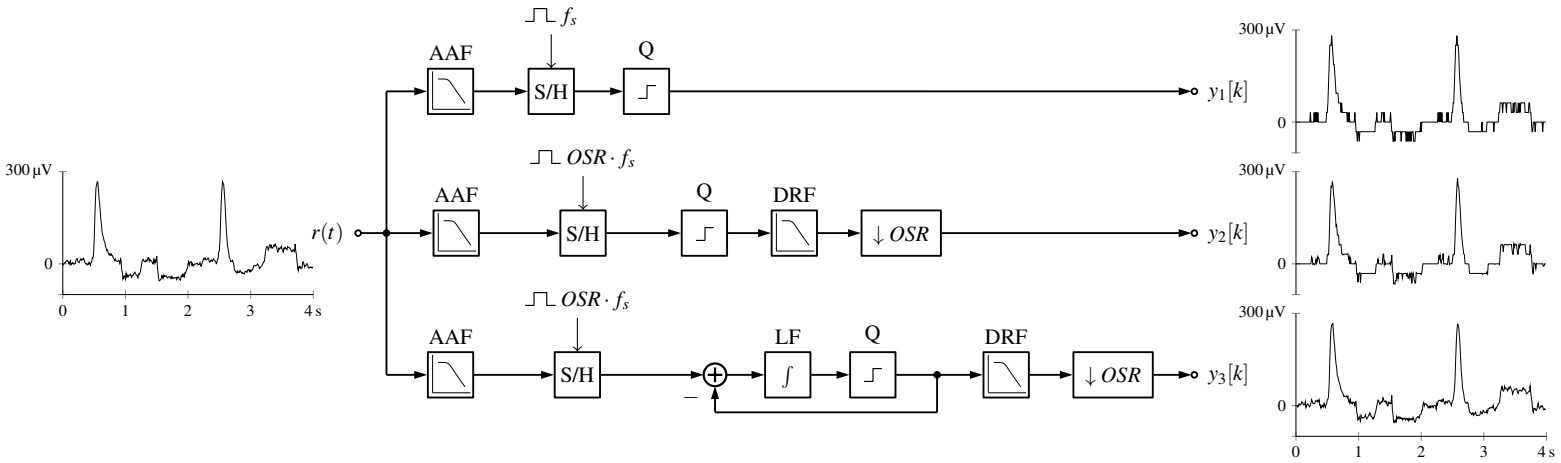

Figure 1.2: A comparison between naïve quantization (top), 10 times oversampled quantization (middle), and first order sigma delta modulation (bottom). The graphs on the right show the increasing quality of an EEG signal [1] sampled to a final rate of 100 Hz and quantized by Q with 5 bits by each scheme.

behaviour is implemented by wrapping the filter and quantizer in a feedback loop. With the same white noise assumption, the tradeoff between in-band shaped quantization noise and OSR is improved for ideal loop filters when order n is increased as shown in Equation 1.2 [2]. The effect of oversampling and noise shaping is demonstrated in Figure 1.2.

$$P_Q = \frac{\Delta^2 \pi^{2n}}{12\,(2n+1) \cdot OSR^{2n+1}} \tag{1.2}$$

1.2 Basic Structure

We introduce the basic block diagram of a sigma delta modulator and nomenclature that will be used herein. For brevity, we limit the scope to sigma delta A/D converters but the concepts are easily transferrable to the D/A case. Modulators can be one of two main classes, CT or DT referring to the nature of the loop filter (LF).

1.2.1 Discrete-Time Modulator

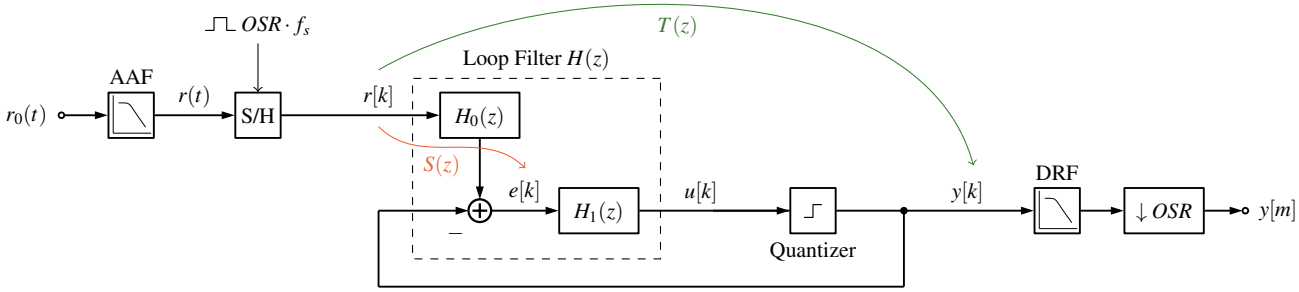

Figure 1.3: The basic block diagram of a DT sigma delta A/D converter.

For the DT class of modulators, we reference Figure 1.3. The analog front-end includes the AAF and sample-and-hold block. This subsystem conditions the input signal $r_0(t)$ and samples it outside the loop to produce DT signal $r[k]$. In the modulator loop, the 2-input 1-output LF operates on $r[k]$ and the feedback signal, producing intermediate signal $u[k]$ with shaped noise. Then, $u[k]$ undergoes quantization producing discrete-value output $y[k]$. The quantizer output is fed back to the LF and also passed along. The final subsystem filters the signal from the shaped noise in the digital domain with a downsampling DRF to yield the final digital output $y[m]$.

From a control systems perspective, there are a couple of transfer functions that will be used to analyze and synthesize loop filters. The sensitivity function $S(\lambda)$, where $\lambda = z$, is known as the noise transfer function (NTF) of the modulator because it shows how the quantization error is filtered in the linearized model. The complementary sensitivity function $T(\lambda)$ is known as the signal transfer function (STF) of the modulator and shows how the signal is transformed by the modulator loop.

1.2.2 Continuous-Time Modulator

For the CT class of modulators, we reference Figure 1.4. The structure is similar except the LF operates directly on analog input $r(t)$ in the CT domain and sampling is done inside the loop. The AAF is no longer necessary in most cases as the LF

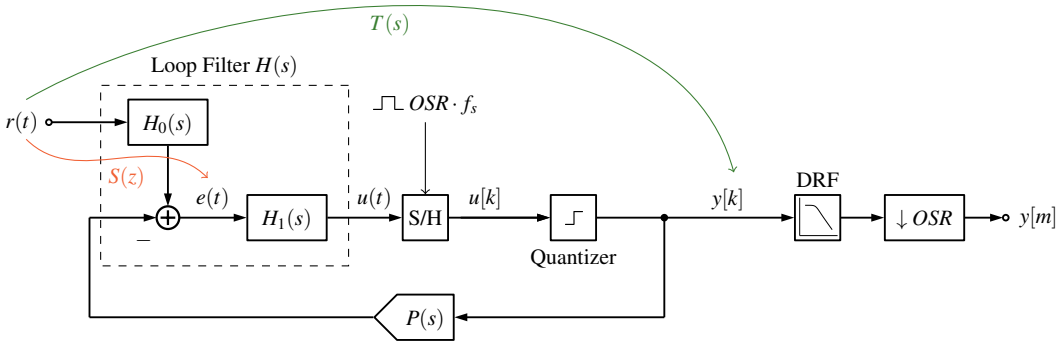

Figure 1.4: The basic block diagram of a CT sigma delta A/D converter.

precedes the sampling block and implicitly attenuates components of the signal that would result in aliasing. Finally, signal $y[k]$ must undergo D/A conversion during feedback, modelled witht the pulse transfer function $P(s)$.

The NTF and STF of a CT sigma delta modulator are more difficult to define because they are transfer functions involving both CT and DT signals. The DT equivalence principle states that there is a DT modulator model that exactly describes the CT design at the sampling instants, because the modulator is overall a sampled data system [3, Sec. 3.2]. Thus, DT transfer functions can be derived for this purpose. However, these equivalent transfer functions may be difficult to manipulate due to their dependence on $P(s)$. For the purposes of this thesis, we omit the sampling block during design and use the simplification that $S(\lambda)$ and $T(\lambda)$ are CT ($\lambda = s$) transfer functions mapping $t(t) \rightarrow e(t)$ and $r(t) \rightarrow y(t)$, respectively.

1.3 Loop Filter

Together, quantization and noise shaping permit a coarser quantizer element to be used. A common design pattern is to use a high (> 2) order LF paired with a 1-bit quantizer, which is advantageous from a circuit design perspective because a quantizer with just two levels is inherently linear. In addition, low order sigma delta loops often suffer from spurious tones [4, Sec. 2.6.1]. Unfortunately, as LF order is increased, the tendency of the loop to become unstable does as well. While first

and second order designs are provably stable for DC inputs [5], high order filters require careful design to avoid instability. Ensuring stability while maintaining performance is a difficult task due to the presence of the highly nonlinear quantizer. Note that the nonlinearity makes analysis complicated, a stable linear model does not imply a stable modulator while an unstable model can even result in a stable modulator [6].

The design of the noise shaping loop filter is the focus of this thesis. Modelling the loop filter as a 2-input 1-output system as shown in Section 1.2 allows the NTF to be determined by $H_1(\lambda)$ alone while the STF can be modified independently with filter $H_0(\lambda)$, without loss of generality:

$$S(\lambda) = \frac{1}{1 - H_1(\lambda)} \tag{1.3}$$

$$T(\lambda) = \frac{H_0(\lambda)}{1 - H_1(\lambda)}. \tag{1.4}$$

We desire an NTF that results in a stable linear model, rejects noise in the signal band as much as possible, and has low gain in the out-of-band region to promote stability. The STF is less important as $H_0(\lambda)$ can be interpreted as a pre-filter to modify the STF, but we prefer unity gain in the signal band.

For a first order modulator, a pure integrator can be used as the loop filter $H_0(\lambda)$. For higher orders, it is common to choose a prototype NTF from a family of filters. For example, the popular Delta Sigma Toolbox for MATLAB [4, Appx. B] uses a Chebyshev type II filter for this purpose. The choice of filter greatly affects the stability of the loop, so the traditional design procedure involves extensive simulation under varying input conditions to ensure instability is unlikely during normal operation. Once unstable, the filter states must be reset in order to restore operation. Various schemes to detect the onset of instability [7] and avoid it with gain scaling [8], internal linear feedback [9], and automatic resetting schemes [10].

1.4 Related Works

Optimization techniques have been used to design NTFs with more degrees of freedom than those made with a single filter prototype. A simple example is that from

[4, Sec. 4.3], where the zeros of the prototype NTF are optimized by approximating the integral of the NTF in the pass-band, then minimizing it analytically by equating its derivative to zero. The procedure results in an optimal spreading of zeros across the signal bandwidth for the given NTF poles. One of the first optimization-based approaches to NTF design was the closed-loop analysis of noise shaper (CLANS) methodology that minimizes P_Q under the white quantization noise assumption [11]. This is done using nonlinear optimization to find stable NTF pole locations that minimize the accumulation of quantization error subject to some stability and realizability constraints.

Using the principles from $\mathscr{H}_\infty$ control and its associated linear matrix inequality (LMI) methods, one can define the quantizer as a very simple feedthrough plant and introduce weighting filters on the feedback error signal e, loop filter output u, and quantizer output y to design the loop filter as a controller for various performance and stability constraints [12]. However, the system is bound to the order of the plant augmented with weighting filters and relies on the designer to choose the weights. Choosing weighting filters that are ideal is almost as difficult a task as just choosing the prototype NTF directly. Despite this, if a known AAF or DRF is specified in advance, it may be used as a sort of weighting filter and an optimal LF can be designed around it [13]. Applications for this method could be optimizing the STF to a psychoacoustic model or making use of existing filters in the signal path.

More recently, the generalized Kalman-Yakubovič-Popov (GKYP) lemma has been applied to sigma delta modulator design. The lemma provides a link between a finite frequency domain inequality, such as specifications on the NTF gain, and a linear matrix inequality condition, which can be solved using efficient interior point methods. Using this lemma, the techniques of $\mathscr{H}_\infty$ control can be applied to a transfer function but restricted to a frequency band. This eliminates the need for weighting filters that specify a select band of interest. Unfortunately, the problem becomes non-convex and hard to solve if both poles and zeros are to be optimized simultaneously as is the case with an infinite impulse response (IIR) filter. As a workaround, the NTF poles may be fixed to a prototype design and just the zeros optimized [14], similar to what was described above. Alternatively, a finite impulse response (FIR) NTF form may be assumed [15, 16] then possibly converted to IIR

form using approximate methods such as least-squares or Yule-Walker [17]. Aside from the large delay introduced, the FIR form is not the optimal choice according to [18]. Iterative methods have shown promise in providing a workaround to the non-convexity associated with direct IIR design. A survey of some of these methods is presented in [19].

1.5 Organization of this Thesis

Having established some background on the workings and nomenclature of a sigma delta modulator, we expand upon this in Chapter 2 to show modifications to the general sigma delta model based on control theory that will permit it to be used in an optimization framework. In Chapter 3, we introduce various stability criteria ranging from heuristics to sufficient conditions and their impact on performance. Following the discussion of the role of optimization in loop filter design, Chapter 4 bridges the model and stability criteria chapters by introducing a semidefinite programming framework that supports the aforementioned criteria. The design process is discussed in Chapter 5, with emphasis on simulation results as well as an empirical study of the tradeoff between performance and stability when designing to different criteria. Finally, we conclude in Chapter 6 with some discussion about the merits and shortcomings of this method of sigma delta modulator design and possible directions for future work.

Chapter 2

Modelling the Sigma Delta Modulator

In order to apply an optimization framework to the design of the LF, the system from Figures 1.3 and 1.4 must be placed in a form that allows tractable application of the desired performance and stability targets. This includes omission of blocks that have minimal or no effect on the loop as well as linearization of the quantizer. The AAF (when present) can be considered as a pre-filter operating on the input signal. The filter $H_0(\lambda)$ serves as an additional degree of freedom for the STF can be set to unity for the purposes of the model. These two filters are not required in stabilitiy analysis, because the NTF depends only on $H_1(\lambda)$ as seen in Equation 1.4. After noise rejection performance has been optimized, $H_0(\lambda)$ can be tuned as necessary to ensure that the combined gain of the AAF and LF is close to unity in the signal band. In a similar way, the digital signal processing (DSP) in the output path serves only to filter out the signal and decimate to the original sampling frequency which may be dealt with separately without impacting loop stability.

2.1 Linearization of the Quantizer Element

Next, the nonlinear nature of the quantizer is dealt with. As mentioned before, a common linearization approach is to replace the quantizer with an additive noise source d. Furthermore, the linear model can incorporate a variable gain K. The

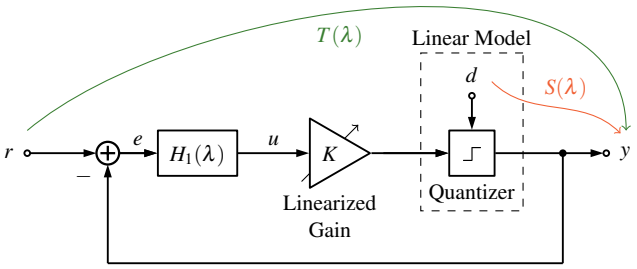

Figure 2.1: The linearized sigma delta loop block diagram with omission of extraneous filters and the quantizer replaced by a variable gain and additive quantization noise signal.

inclusion of K has uses in linearization, stability, and performance that will be expanded upon in Chapter 3. After these simplifications, we obtain the block diagram in Figure 2.1 which is applicable to DT or CT designs. In the DT case, the loop is operating entirely in the oversampled domain and the sample-and-hold (S/H) block is not shown. In the CT case, the S/H block in the loop is neglected so that $S(\lambda)$ and $T(\lambda)$ are CT transfer functions[1].

2.2 Well-Posedness and Internal Stability

The meaningful application of feedback to reduce an uncertainty (in this case, error introduced by the nonlinear quantizer) requires that the system be well-posed in order for a solution to exist. Figure 2.1 can undergo block diagram mainpulation bringing it into the standard feedback form shown in Figure 2.2 with signals r, e, d, and y.

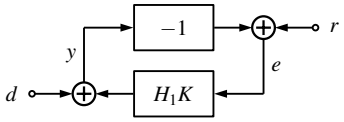

Figure 2.2: The linearized model converted into standard feedback form.

[1]Note that regarding Figure 2.1 and Figures 1.3/1.4, the NTF $S(\lambda)$ is the same transfer function whether interpreted from $d \to y$ or $r \to e$.

The equations describing this loop are:

$$\begin{bmatrix} r \\ d \end{bmatrix} = \begin{bmatrix} 1 & 1 \\ -H_1K & 1 \end{bmatrix} \begin{bmatrix} e \\ y \end{bmatrix}. \tag{2.1}$$

A feedback system is considered well-posed if the inverse of the transfer matrix in Equation 2.1 exists and each of its elements are proper. Equation 2.2 shows that this is the case if both $S(\lambda)$ and $T(\lambda)$ are proper transfer functions.

$$\begin{bmatrix} e \\ y \end{bmatrix} = \begin{bmatrix} 1 & 1 \\ -H_1K & 1 \end{bmatrix}^{-1} = \begin{bmatrix} \frac{1}{1+H_1K} & \frac{-1}{1+H_1K} \\ \frac{H_1K}{1+H_1K} & \frac{1}{1+H_1K} \end{bmatrix} \begin{bmatrix} r \\ d \end{bmatrix} = \begin{bmatrix} S & -S \\ T & S \end{bmatrix} \begin{bmatrix} r \\ d \end{bmatrix}. \tag{2.2}$$

The principle of internal stability is stricter than bounded-input bounded-output (BIBO) stability because it guarantees that the internal states of the system remain bounded. The system in Equation 2.2 is internally stable if each element of the transfer matrix belongs to the set $\mathscr{RH}_\infty$, that is the set of stable real rational proper transfer functions.

2.2.1 Constraints on the Noise Transfer Function

A sufficient condition for $S(\lambda)$ and $T(\lambda)$ to be proper is that transfer function $H_1(\lambda)$ is a strictly proper real rational transfer function. Internal stability of the system follows if $S(\lambda)$ and $T(\lambda)$ are stable. This leads to the following constraints on the NTF:

1. $S(\lambda)$ is stable, and ,
2. The following equivalent conditions hold:
   (a) $S(\infty) = 1$,
   (b) If $S(\lambda)$ is in state-space form, the feedthrough matrix $D = 1$, and,
   (c) The first element of the impulse response of $S(\lambda)$ is one.

Most prior work in the area performs optimization directly on the NTF of the system. This is effective because it is a relatively accurate model of the noise

shaping performance. In addition, constraint 2 enforces causality on the feedback loop ensuring the system is physically realizable.

2.3 Modelling Uncertain Quantizer Gain

Having established conditions to ensure the closed-loop system is realizable and internally stable, we must focus on the variable gain K. K can be understood as a time-varying gain dependent on the quantizer input. For example, a 1-bit quantizer ($\Delta = 2$) with output $\{-1, 1\}$ would have instantaneous gain $K(t) = \frac{1}{u(t)}$. As the value of u at each sample time is not known in advance, we model K as a multiplicative uncertainty. The upper linear fractional transformation (LFT) allows K to be separated into a constant gain matrix $M_{2\times 2}$ and a normalized, $\mathscr{H}_\infty$ norm-bounded uncertain block Δ by Expression 2.3.

$$K \leftrightarrow \mathscr{F}_U\{M, \Delta\} \quad ||\Delta||_\infty \leq 1 \tag{2.3}$$

The model from Figure 2.2 is shown in Figure 2.3 with the quantizer and variable gain replaced by this LFT interconnection. In Chapter 4, we are interested in ensuring the robustness of the system to Δ, which may be achieved using this form.

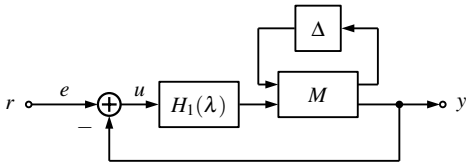

Figure 2.3: The linearized block diagram with the quantizer replaced by a multiplicative uncertainty extracted via LFT.

2.4 Derivation of Augmented System

2.4.1 Extraction of Performance and Stability Channels

Finally, we abstract the model into an augmented form where all desired input and output channels are present and all unnecessary ones hidden. Let the LFT input to M and output from M be w and z, respectively. These channels are required to

Input \ Output	z	e	u	y
r	Not used	NTF performance channel	Constraint on quantizer input signal	STF constraints for CT design
w	Quantizer gain robustness channel	Not used	Not used	Not used

Table 2.1: Input and output channels of interest for the augmented system.

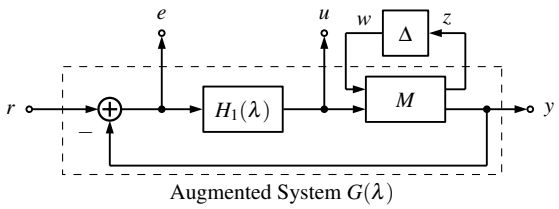

Figure 2.4: The augmented plant is derived by setting $H_0(\lambda) = 1$, taking the LFT of the uncertain gain, extracting the signals of interest, and writing the closed-loop equations.

be accessed in addition to r, e, u, and y for the purposes listed in Table 2.1. The augmented system $G(\lambda)$ is shown as the dashed block in Figure 2.4.

2.4.2 Derivation of State-Space Model

Now that the desired input and output signals are captured by the model, it is a simple exercise to write the system in state-space form. To begin, let filter $H_1(\lambda)$ be the transfer function of order n in variable $\lambda = z$ in the DT case (or $\lambda = s$ in the CT case). The numerator and denominator coefficients are shown in Equation 2.4 which has the equivalent state-space representation of Equation 2.5.

$$H_1(\lambda) = \frac{b_{n-1}\lambda^{n-1} + b_{n-2}\lambda^{n-2} + \ldots + b_1\lambda + b_0}{\lambda^n + a_{n-1}\lambda^{n-1} + a_{n-2}\lambda^{n-2} + \ldots + a_1 z\lambda + a_0} \tag{2.4}$$

$$= C_H(\lambda I - A_H)^{-1}B_H \tag{2.5}$$

Naturally, $H_1(\lambda)$ is a strictly proper transfer function and state-space feedthrough matrix $D_H = 0$ due to the constraints proposed in Section 2.2. The constant gain matrix M may be split into its constituent parts as shown in Equation 2.6.

$$M = \begin{bmatrix} m_{11} & m_{12} \\ m_{21} & m_{22} \end{bmatrix} \tag{2.6}$$

With some algebra, the augmented system $G(\lambda)$ from Figure 2.4 may be written in state-space form with notation from Equations 2.5 and 2.6 by introducing state vector x. We use the notation $G_{qp}(\lambda)$ to indicate the transfer function of $G(\lambda)$ from some input channel p to some output channel q and name the closed-loop state-space matrix blocks with cursive letters as shown in Equation 2.8.

$$G: \begin{bmatrix} \dot{x} \\ z \\ e \\ u \\ y \end{bmatrix} = \left[\begin{array}{c|cc} A_H - m_{22}B_HC_H & -m_{21}B_H & B_H \\ \hline m_{12}C_H & m_{11} & 0 \\ -m_{22}C_H & -m_{21} & 1 \\ C_H & 0 & 0 \\ m_{22}C_H & m_{21} & 0 \end{array}\right] \begin{bmatrix} x \\ w \\ r \end{bmatrix} \tag{2.7}$$

$$= \left[\begin{array}{c|cc} \mathscr{A} & \mathscr{B}_w & \mathscr{B}_r \\ \hline \mathscr{C}_z & \mathscr{D}_{zw} & \mathscr{D}_{zr} \\ \mathscr{C}_e & \mathscr{D}_{ew} & \mathscr{D}_{er} \\ \mathscr{C}_u & \mathscr{D}_{uw} & \mathscr{D}_{ur} \\ \mathscr{C}_y & \mathscr{D}_{yw} & \mathscr{D}_{yr} \end{array}\right] \begin{bmatrix} x \\ w \\ r \end{bmatrix} \tag{2.8}$$

With the channels of interest exposed and the system in a state-space form, we must now express design goals as constraints on these channels. In Chapter 3, we discuss various stability measures and performance goals and select those which are ideal for an optimization perspective. In Chapter 4, the framework is introduced to allow the targets from the previous chapter to be applied to the augmented system in a way that allows the optimization problem to be efficiently solved.

Chapter 3

Stability Criteria and Performance Goals

3.1 Stability Concepts Not Used by this Optimization Framework

3.2 Stability Criteria Used by this Optimization Framework

Chapter 4

Optimization of Loop Filter Design

Chapter 5

Design Examples

Chapter 6

Conclusions

Bibliography

[1] B. Blankertz, G. Dornhege, M. Krauledat, K. R. Müller, and G. Curio, "The non-invasive Berlin Brain-Computer Interface: Fast acquisition of effective performance in untrained subjects," *Neuroimage*, vol. 37, no. 2, pp. 539–550, 2007. → pages ix, 3

[2] J. M. De La Rosa, "Sigma-delta modulators: Tutorial overview, design guide, and state-of-the-art survey," *IEEE Trans. Circuits Syst. I Regul. Pap.*, vol. 58, no. 1, pp. 1–21, 2011. → pages 2, 3

[3] M. Ortmanns and F. Gerfers, *Continuous-Time Sigma-Delta A/D Conversion*. 2005. → page 5

[4] R. Schreier and G. C. Temes, *Understanding Delta-Sigma Data Converters*, vol. 53. Wiley, 1997. → pages 5, 6, 7

[5] S. Hein and A. Zakhor, "On the Stability of Sigma Delta Modulators," *IEEE Trans. Signal Process.*, vol. 41, no. 7, pp. 2322–2348, 1993. → page 6

[6] L. Risbo, *Sigma Delta Modulators - Stability Analysis and Optimization*. Doctor of philosophy, Technical University of Denmark, 1994. → page 6

[7] N. Wong and T.-s. Ng, "Fast detection of instability in sigma-delta modulators based on unstable embedded limit cycles," *IEEE Trans. Circuits Syst. II*, vol. 51, no. 8, pp. 442–449, 2004. → page 6

[8] N. S. Sooch, "Gain Scaling of Oversampled Analog-to-Digital Converters," 1989. → page 6

[9] S. M. Moussavi and B. H. Leung, "High-Order Single-Stage Single-Bit Oversampling A/D Converter Stabilized with Local Feedback Loops," *IEEE Trans. Circuits Syst.*, vol. 41, no. 1, pp. 19–25, 1994. → page 6

[10] F. O. Eynde, G. M. Yin, and W. Sansen, "A CMOS Fourth-order 14b 500k-sample/s Sigma-delta ADC Converter," 1991. → page 6

[11] J. Kenney and L. Carley, "CLANS: a high-level synthesis tool for high resolution data converters," in *IEEE Int. Conf. Comput. Des. Dig. Tech. Pap.*, (Pittsburgh), pp. 496–499, 1988. → page 7

[12] A. Oberoi, *A Convex Optimization Approach to the Design of Multiobjective Discrete Time Systems*. Master of science, Rochester Institute of Technology, 2004. → page 7

[13] S. Ohno and M. Rizwan Tariq, "Optimization of Noise Shaping Filter for Quantizer with Error Feedback," *IEEE Trans. Circuits Syst. I Regul. Pap.*, vol. 64, no. 4, pp. 918–930, 2017. → page 7

[14] M. M. Osqui and A. Megretski, "Semidefinite Programming in Analysis and Optimization of Performance of Sigma-Delta Modulators for Low Frequencies," in *Proc. 2007 Am. Control Conf.*, no. 6, pp. 3582–3587, 2007. → page 7

[15] M. Nagahara and Y. Yamamoto, "Frequency Domain Min-Max Optimization of Noise-Shaping Delta-Sigma Modulators," *IEEE Trans. Signal Process.*, vol. 60, no. 6, pp. 1–12, 2012. → page 7

[16] M. R. Tariq and S. Ohno, "Unified LMI-based design of ΔΣ modulators," *EURASIP J. Adv. Signal Process.*, vol. 2016, no. 1, p. 29, 2016. → page 7

[17] M. R. Tariq, S. Ohno, and M. Nagahara, "Synthesis of IIR error feedback filters for ΔΣ modulators using approximation," in *2016 Asia-Pacific Signal Inf. Process. Assoc. Annu. Summit Conf. APSIPA 2016*, (Jeju), pp. 7–11, 2017. → page 8

[18] M. S. Derpich, E. I. Silva, D. E. Quevedo, and G. C. Goodwin, "On optimal perfect reconstruction feedback quantizers," *IEEE Trans. Signal Process.*, vol. 56, pp. 3871–3890, aug 2008. → page 8

[19] S. Callegari and F. Bizzarri, "Optimal design of the noise transfer function of ΔΣ modulators: IIR strategies, FIR strategies, FIR strategies with preassigned poles," *Signal Processing*, vol. 114, pp. 117–130, 2015. → page 8

Appendix A

Supporting Materials

This would be any supporting material not central to the dissertation. For example:

- additional details of methodology and/or data;
- diagrams of specialized equipment developed.;
- copies of questionnaires and survey instruments.